YMTHE, Volume *30*

Supplemental Information

Type I IFNs repolarized a CD169^{+} macrophage population with anti-tumor potentials in hepatocellular carcinoma

Jing Liao, Dan-Ni Zeng, Jin-Zhu Li, Qiao-Min Hua, Chun-Xia Huang, Jing Xu, Chong Wu, Limin Zheng, Wei-Ping Wen, and Yan Wu

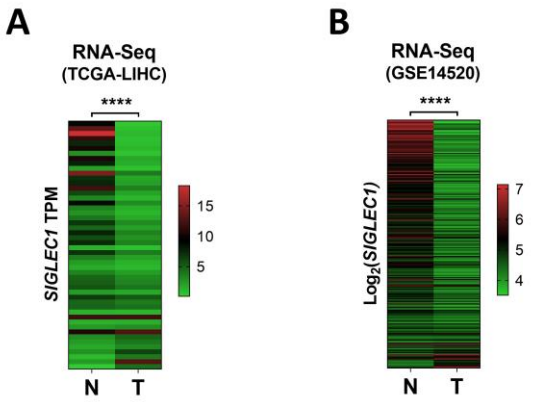

Supplementary Figure 1. *SIGLEC1* mRNA expression in HCC tissues

(**A**) *SIGLEC1* mRNA expression of 50 paired non-tumor (N) and tumor (T) liver hepatocellular carcinoma (HCC) samples from TCGA data set. (**B**) *SIGLEC1* mRNA expression of 234 paired non-tumor and tumor HCC samples from GSE14520 data set.

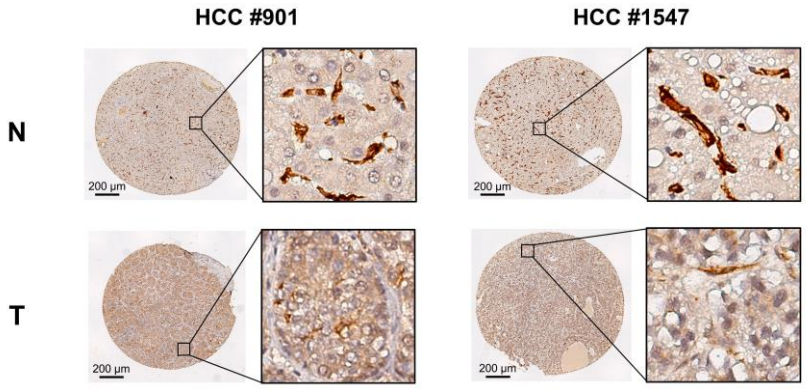

Supplementary Figure 2. Representative immunohistochemical staining of CD169 in HCC tissue microarray

Representative images of immunohistochemistry analyses of CD169 (strong brown staining) in HCC nontumoral and tumoral tissues.

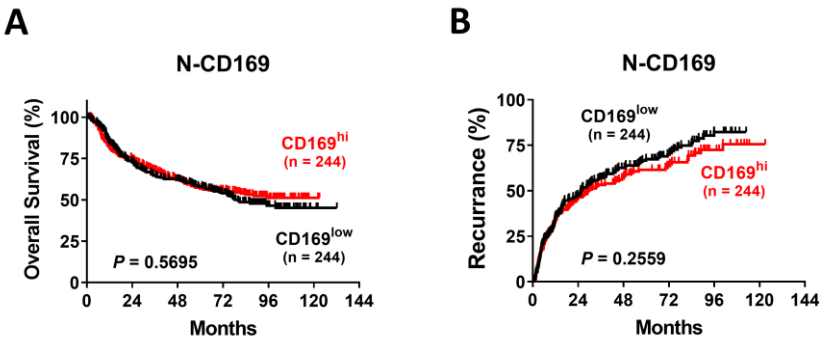

Supplementary Figure 3. Level of non-tumor infiltrating CD169$^+$ Mφ is not associated with disease progression

(A-B) 488 HCC patients were divided into two groups according to the median of the CD169$^+$ cells density in nontumor regions. The cumulative overall survival (A) and recurrence (B) was calculated using the Kaplan-Meyer method and then analyzed with the log-rank test.

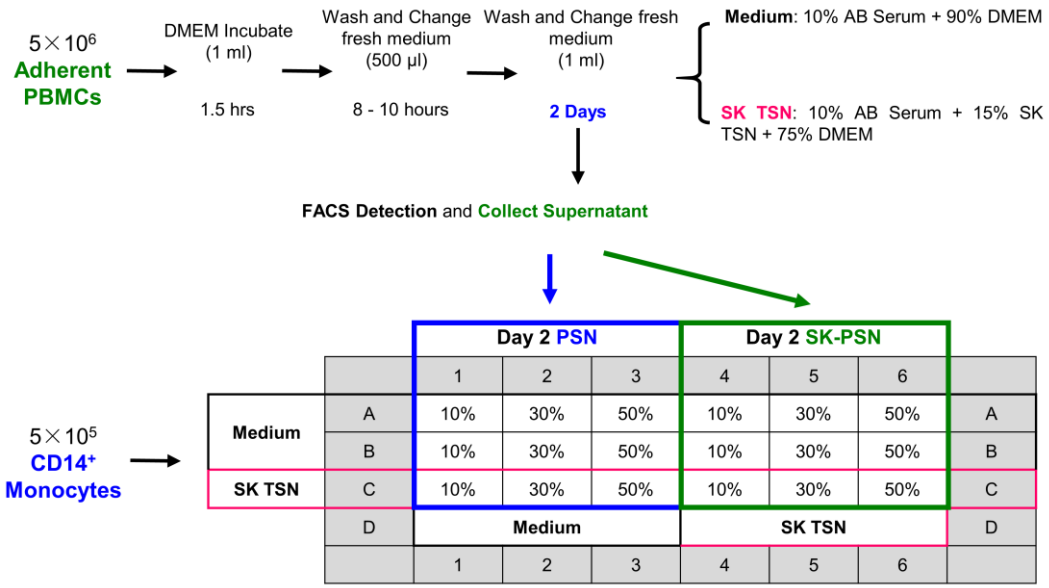

		1	2	3	4	5	6	
Medium	A	10%	30%	50%	10%	30%	50%	A
	B	10%	30%	50%	10%	30%	50%	B
SK TSN	C	10%	30%	50%	10%	30%	50%	C
	D	Medium			SK TSN			D
		1	2	3	4	5	6	

Supplementary Figure 4. Procedure of collecting SK TCS -treated PBMCs condition supernatants

PBMCs enrichment by adherent treatment method were precultured with medium or SK TCS, and supernatants (PSN or SK-PSN) were collected at 48 hours. Thereafter, $CD14^{+}$ monocytes were isolated with magnetic bead sorting, and cultured with the indicated supernatants for 48 hours.

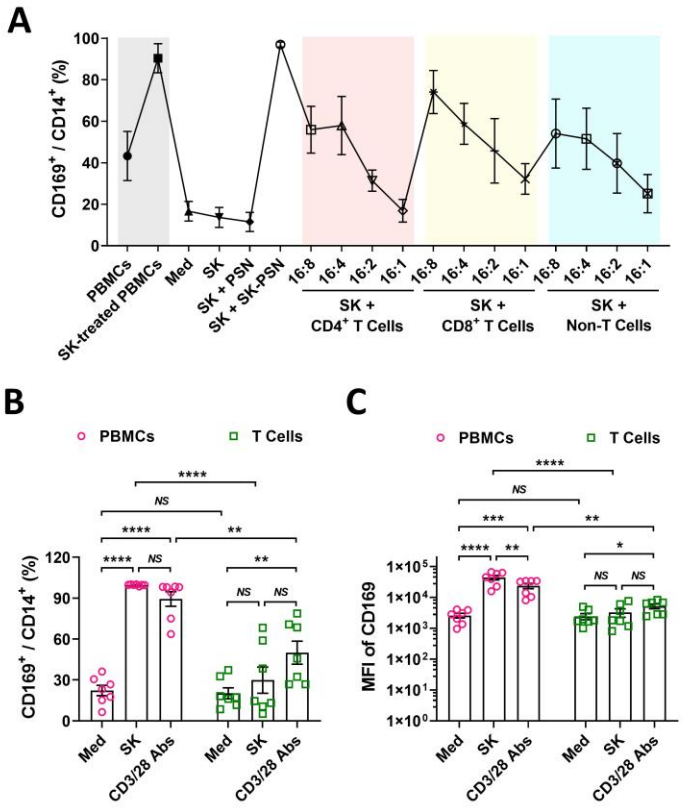

Supplementary Figure 5. Activated T lymphocytes-derived soluble factors are responsible for CD169 induction on monocytes

(**A**) Dark region: PBMCs enrichment by adherent method were cultured with medium or SK TCS. Other regions: monocytes were isolated from PBMCs of healthy donor using CD14 beads, and $CD4^+$ T cells ($CD14^-CD19^-CD4^+CD8^-$), $CD8^+$ T cells ($CD14^-CD19^-CD4^-CD8^+$), non-T cells ($CD14^-CD19^-CD4^-CD8^-$) were sorted by flow cytometry. $CD14^+$ monocytes (5×10^5) were cocultured with or without sorted cells in various condition. Two days later, the ratio of $CD169^+$ cells in $CD14^+$ cells were determined by flow cytometry, n = 5. (**B-C**) PBMCs (5×10^6 cells/ml) enrichment by adherent method were pretreated in the presence of medium, SK TCS (30%), or CD3/28 antibodies (2 μg/ml anti-CD3 antibody and 4 μg/ml anti-CD28 antibody), respectively. $CD3^+$ T cells (1×10^6 cells/ml) sorted by flow cytometry were pretreated in the presence of medium (40 U/ml IL-2), SK TCS (30% TCS and 40 U/ml IL-2), or CD3/28 antibodies (40 U/ml IL-2, 2 μg/ml anti-CD3 antibody coating, and 4 μg/ml anti-CD28 antibody), respectively. Supernatants were collected at 2 days later, and $CD14^+$ monocytes (5×10^5) were cocultured with 30% indicated supernatants. Two days later, the ratio of $CD169^+$ cells in $CD14^+$ cells (b) and the MFI of CD169 on $CD14^+$ cells (c) were determined by flow cytometry, n = 7. Data represent mean ± SEM; *NS*, no significant; **P* < 0.05; ***P* < 0.01; *****P* < 0.0001; Two-way ANOVA multiple comparisons (b and c).

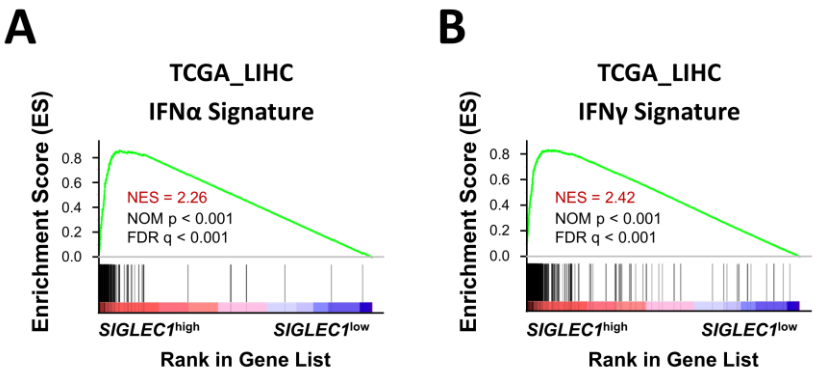

Supplementary Figure 6. CD169 reflects IFN signatures in human HCC

(**A-B**) GSEA of IFNα signature (A) and IFNγ signature (B) in 183 *SIGLEC1*^{high} and 182 *SIGLEC1*^{low} counterparts from TCGA data set. The enrichment scores, NOM p values and FDR q values were calculated by GSEA with weighted enrichment statistics and ratio of classes for the metric as input parameters.

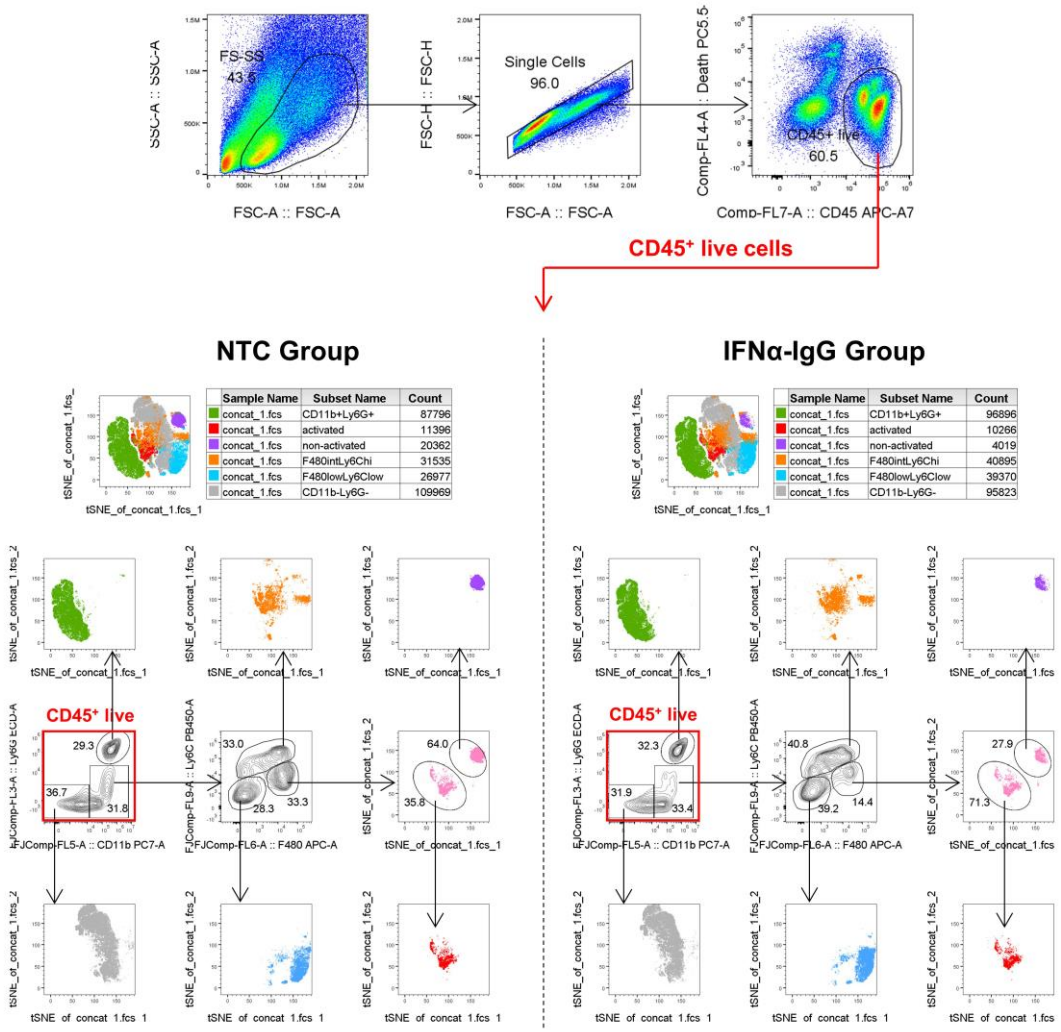

Supplementary Figure 7. Gating strategies

WT C57B/6 mice were injected subcutaneously with 1×10^6 Hepa1-6 cells. Then, 10 μg of IFNα-IgG or PBS (no treatment control, NTC) was administered intravenously on day 8, and tumor tissues were collected on day 11, n = 10. Multiparametric flow cytometry analysis was performed of live immunocytes isolated from freshly dissociated tumor specimens.

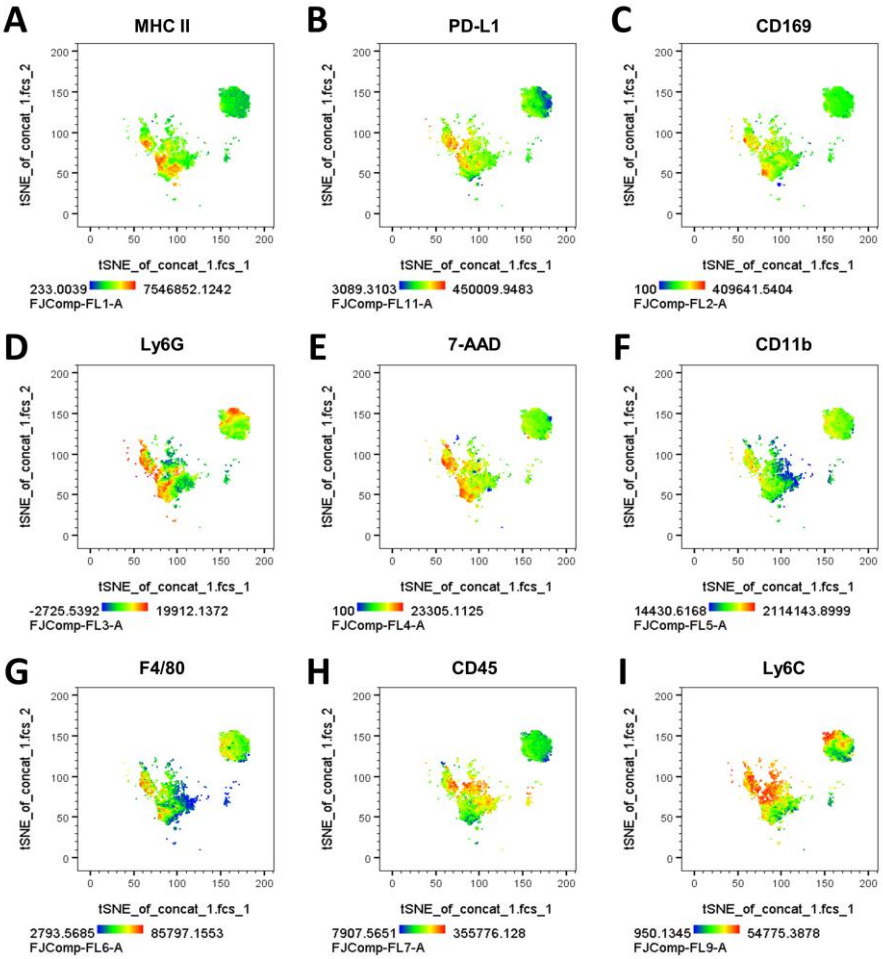

Supplementary Figure 8. Heatmap of various molecular expression between F4/80^{hi}Ly6C^{int} – act and F4/80^{hi}Ly6C^{int} – non-act clusters

(**A-I**) WT C57B/6 mice were injected subcutaneously with 1 × 10^6 Hepa1-6 cells. Then, 10 μg of IFNα-IgG or PBS (no treatment control, NTC) was administered intravenously on day 8, and tumoral tissues were collected on day 11, n = 10. tSNE plot was displayed for all samples, exhibiting the expression of indicated makers on F4/80^{hi}Ly6C^{int} cluster.

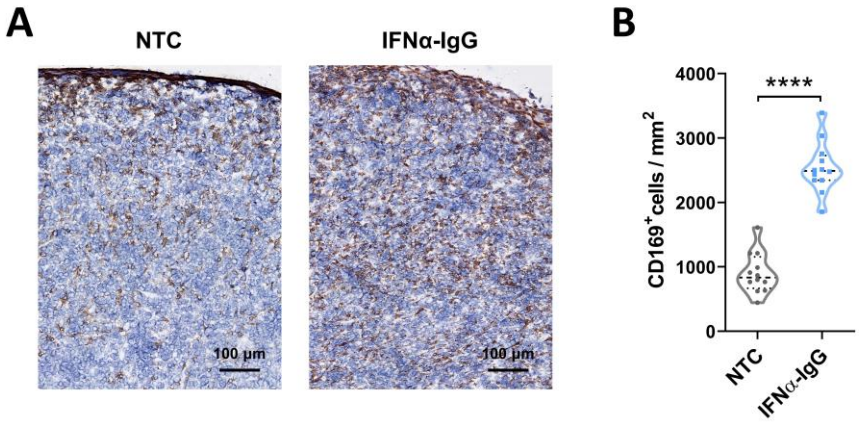

Supplementary Figure 9. Increased CD169$^+$ Mφ infiltration after IFNα-IgG therapy

(**A-B**) WT C57B/6 mice were injected subcutaneously with 1×10^6 Hepa1-6 cells. Then, 10 μg of IFNα-IgG was administered intravenously on day 10, 12 and 14. Tumor tissues were collected on day 21, and immunohistochemical staining of CD169 in frozen tumor sections was performed, n = 3. (A) Representative immunohistochemical staining of CD169 in frozen tumor sections, scale bar = 100 μm. (B) The density of CD169$^+$ cells. Four different views of each section were randomly selected for counting. Data represent violin plot; ****$P < 0.0001$; unpaired Student's *t* test.

Supplementary Tables

Supplementary Table 1. Correlation between clinicopathological parameters and the density of $CD169^+$ cells and $CD8^+$ cells

Characteristics	No. $CD169^+$ (%)			No. $CD8^+$ (%)		
	Low (No. 259)	High (No. 229)	*P* value*	Low (No. 230)	High (No. 257)	*P* value*
Gender						
female	34 (6.97)	22 (4.51)	0.223	33 (6.78)	23 (4.72)	0.062
male	225 (46.11)	207 (42.42)		197 (40.45)	234 (48.05)	
Age, year						
≤ 50	144 (29.51)	95 (19.47)	**0.002**	125 (25.67)	114 (23.41)	**0.028**
> 50	115 (23.57)	134 (27.46)		105 (21.56)	143 (29.36)	
HBsAg						
negative	26 (5.33)	25 (5.12)	0.752	22 (4.52)	29 (5.95)	0.536
positive	233 (47.75)	204 (41.08)		208 (42.71)	228 (46.82)	
AFP, ng/mL						
≤ 25	78 (15.98)	128 (26.23)	**< 0.001**	73 (14.99)	105 (21.56)	**0.037**
> 25	181 (37.09)	101 (20.70)		157 (32.24)	152 (31.21)	
ALT, U/L						
≤ 40	114 (23.36)	132 (27.05)	**0.003**	132 (27.10)	144 (29.57)	0.762
> 40	145 (29.71)	97 (19.88)		98 (20.12)	113 (23.20)	
Cirrhosis†						
absent	49 (10.21)	44 (9.17)	0.997	40 (8.35)	53 (11.06)	0.394
presrent	204 (42.50)	183 (38.13)		185 (38.62)	201 (41.96)	
Differentiation†						
I+II	203 (41.86)	179 (36.91)	0.897	187 (38.64)	194 (40.08)	0.094
III+IV	54 (11.13)	49 (10.10)		41 (8.47)	62 (12.81)	
Tumour multiplicity						
single	182 (37.30)	179 (36.68)	**0.047**	170 (34.91)	190 (39.01)	0.997
multiple	77 (15.78)	50 (10.25)		60 (12.32)	67 (13.76)	
Tumour size, cm						
≤ 5	114 (23.36)	114 (23.36)	0.203	105 (21.56)	123 (25.26)	0.626
> 5	145 (29.71)	115 (23.57)		125 (25.67)	134 (27.52)	
BCLC						
A	154 (31.56)	157 (32.17)	**0.038**	144 (29.57)	166 (34.09)	0.65
B+C	105 (21.52)	72 (14.75)		86 (17.66)	91 (18.69)	
TNM stage						
I+II	168 (34.43)	179 (36.68)	**0.001**	161 (33.06)	185 (37.99)	0.63
III+IV	91 (18.65)	50 (10.25)		69 (14.17)	72 (14.78)	

*$\chi 2$ test. Significant *P* values (< 0.05) are shown in bold.

†Data was missing in these variables for some patients.

Supplementary Table 2. Univariate and multivariate analyses of factors associated with overall survival for HCC

Variables	Overall Survival					
	Univariate Analysis			Multivariate Analysis		
	HR	95% CI	*P* value	HR	95% CI	*P* value
Gender (female *vs.* male)	0.735	0.513-1.054	0.095			
Age, years (≤55 *vs.* > 55)	0.957	0.737-1.243	0.744			
HBsAg (negtive *vs.* positive)	0.996	0.652-1.521	0.985			
AFP, ng/mL (≤25 *vs.* > 25)	1.779	1.333-2.374	**< 0.001**	1.387	1.023-1.880	**0.035**
ALT, U/L (≤40 *vs.* > 40)	1.335	1.029-1.733	**0.030**	1.159	0.883-1.521	0.287
Cirrhosis† (absent *vs.* present)	1.907	1.298-2.800	**0.001**	2.063	1.373-3.100	**< 0.001**
Child-Pugh score (A vs. B)	0.396	0.234-0.669	**0.001**	0.460	0.256-0.829	**0.010**
Differentiation† (I+II vs. III+IV)	1.440	1.065-1.948	**0.018**	1.290	0.928-1.793	0.130
Tumour multiplicity (single vs multiple)	2.142	1.632-2.812	**< 0.001**	1.521	1.008-2.295	**0.046**
Tumour size, cm (≤5 vs. > 5)	1.680	1.286-2.194	**< 0.001**	1.446	1.074-1.948	**0.015**
Vascular invasion (absent vs. present)	5.697	4.093-7.902	**< 0.001**	3.861	2.519-5.918	**< 0.001**
BCLC (A vs. B+C)	3.018	2.321-3.925	**< 0.001**	1.077	0.595-1.948	0.807
TNM stage (I+II vs. III+IV)	3.081	2.364-4.016	**< 0.001**	1.662	0.273-10.126	0.582
T	0.584	0.511-0.667	**< 0.001**	0.756	0.133-4.296	0.752
N	4.213	1.862-9.530	**0.001**	3.270	0.895-11.956	0.073
M	6.036	1.927-18.909	**0.002**	2.270	0.318-16.182	0.413
$CD169_T$ (low vs. high)						
≤122.2 cells/field*	0.424	0.322-0.559	**< 0.001**	0.493	0.364-0.668	**< 0.001**
> 122.2 cells/field*						
$CD8_T$ (low vs. high)						
≤150 cells/field*	0.616	0.474-0.802	**< 0.001**	0.744	0.558-0.993	**0.045**
> 150 cells/field*						

*Each number represents mean value/field of all cases analysed.

Univariate analysis, Cox proportional hazards regression model.

Multivariate analysis, Cox proportional hazards regression model. Variables were adopted by univariate analysis.

Abbreviations: OS, overall survival; DFS, disease-free survival; HR, hazard ratio; CI, confidence interval. N.S., not significant.

†Data was missing in these variables for some patients. *P* values (< 0.05) are shown in bold.

Supplementary Table 3. The definition of gene signatures related with inflamed-cancer

Name	Description
TIDE	Tumor Immune Dysfunction and Exclusion (TIDE) identified factors that underlie these two mechanisms of tumor immune escape. TIDE integrated and modeled data from 189 human cancer studies, comprising a total of 33,197 samples. In totally, there are 23 negative hits.
T cell accumulation	In-vivo shRNA screen in mouse T cells to identify genes whose knockdown can increase the efficiency of T-cell accumulation in tumors. The top 17 hits are defined as genes with a median fold change greater than 2 in the primary screen and larger than one in the validation screen.
T cell exhaustion	Gene expression difference between exhausted CD8 T cells and activated CD8 T cells in a mouse model. The negative hits are defined as the bottom 50 genes ranked by the logFC of differential expression.
T cell regulatory	Gene expression change of CD4 regulatory T cells before and after activation. The negative hits are defined as the bottom 50 genes ranked by the logFC of differential gene expression.
ICB resist	Gene expression difference between anti-CTLA4 resistant mouse tumors and parental sensitive B16 tumors. The negative hits are defined as the bottom 50 genes ranked by the logFC of differential expression.
T cell exhaustion fixed	Gene expression features of exhausted CD8 T cells at different stages. For each time point, we computed a logFC vector testing the gene expression difference between exhausted T cells and naïve T cells. The negative hits are defined as the bottom 50 genes ranked by the logFC of differential expression.
MDSC	Gene expression profiles of myeloid derived suppressor cells that can inhibit T-cell activation compared to monocytes sorted from peripheral blood mononuclear cells. The negative hits are defined as the bottom 50 genes ranked by the logFC of differential expression.
TAM M2/M1	Gene expression profile of M2 macrophages compared to M1 macrophages. The negative hits are defined as the bottom 50 genes ranked by the logFC of differential expression.
CAF	Gene expression profile of FAP^{+} cancer-associated fibroblasts compared to other cell types sorted from the same patients. The negative hits are defined as the bottom 50 genes ranked by the logFC of differential expression.